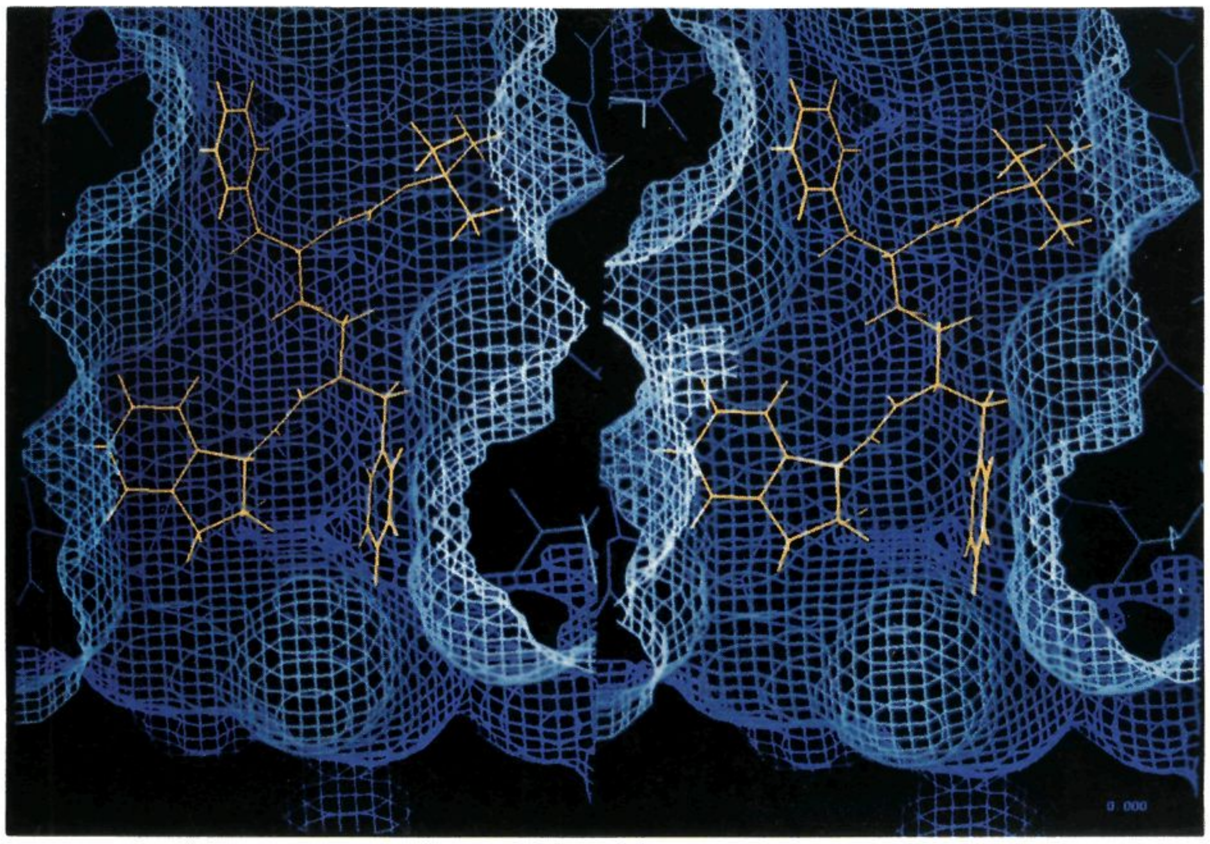

Figure 1. L-685,434 modeled in native HIVP active-site steric surface map.

Scheme I[a]

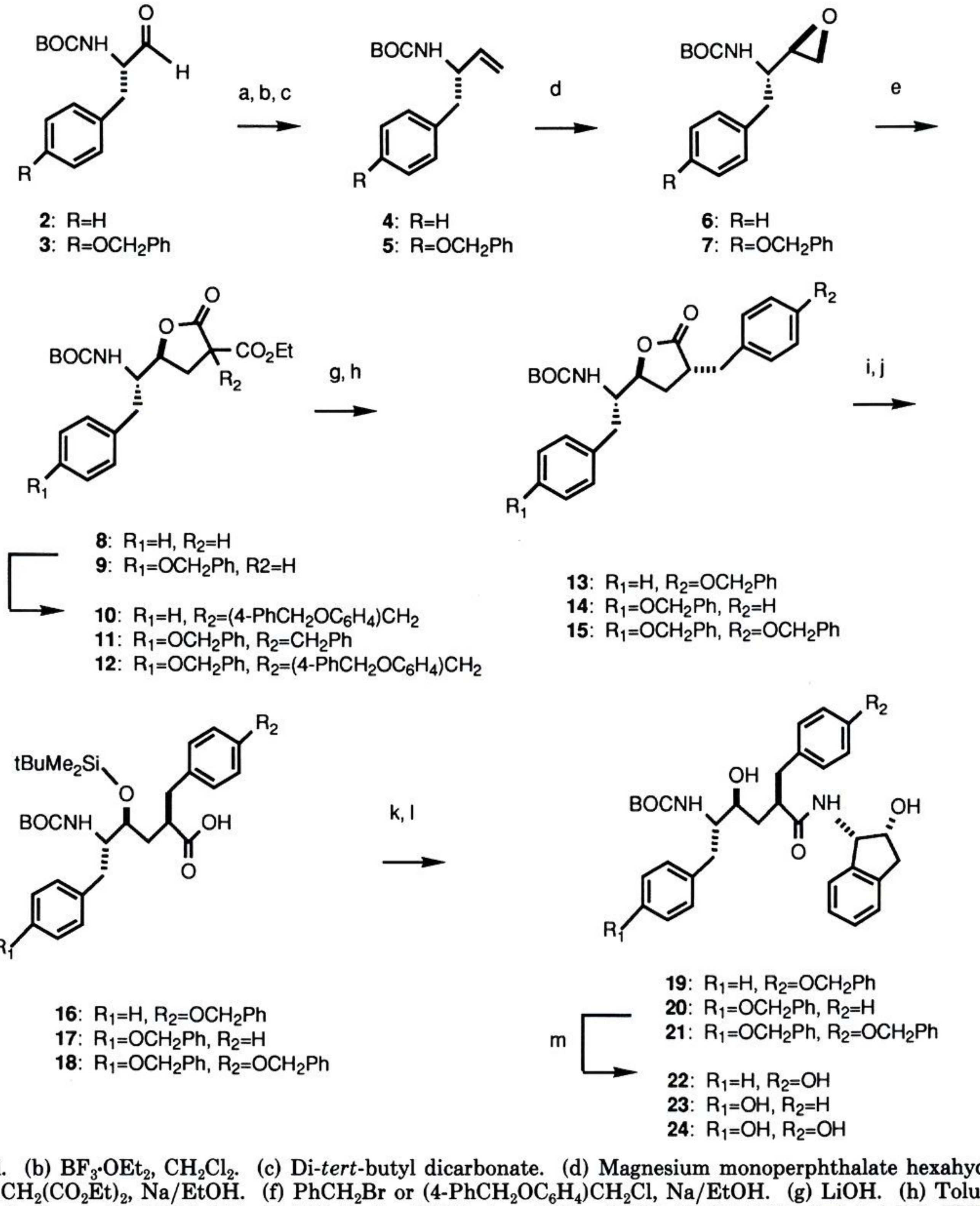

[a] (a) Me_3SiCH_2MgCl. (b) $BF_3{\cdot}OEt_2$, CH_2Cl_2. (c) Di-*tert*-butyl dicarbonate. (d) Magnesium monoperphthalate hexahydrate MeOH or MCPBA, CH_2Cl_2. (e) $CH_2(CO_2Et)_2$, Na/EtOH. (f) $PhCH_2Br$ or $(4\text{-}PhCH_2OC_6H_4)CH_2Cl$, Na/EtOH. (g) LiOH. (h) Toluene, reflux. (i) LiOH. (j) $tBuMe_2SiCl$, imidazole, DMF; MeOH. (k) 1(*S*)-Amino-2(*R*)-hydroxyindan, HOBt, EDC, DMF. (l) $(nBu)_4NF$, THF. (m) H_2, 10% Pd/C, THF–MeOH.

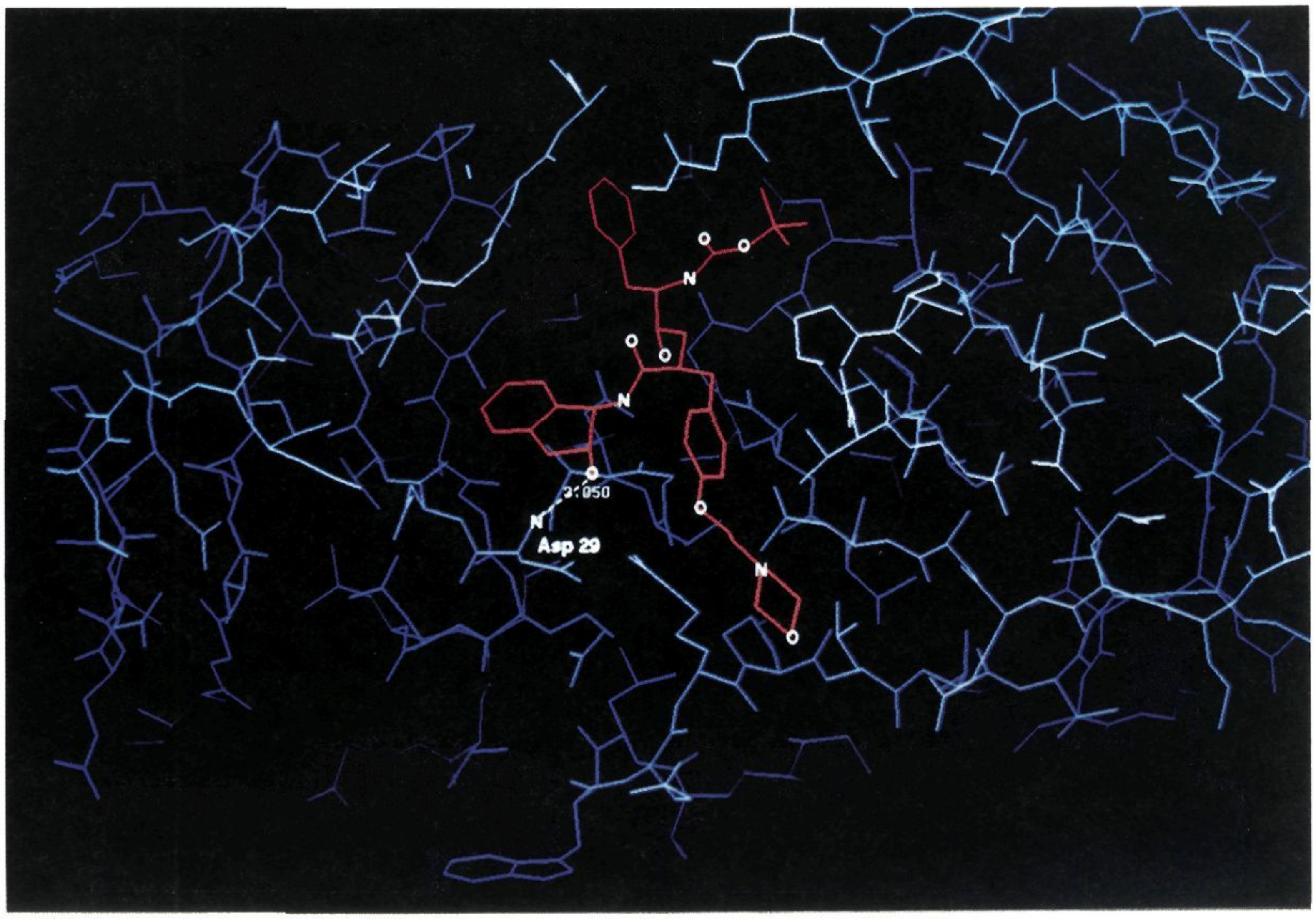

Figure 2. L-689,502 modeled in native enzyme active site.

At the beginning of the structural analysis, it appeared that L-689,502 bound to the nearly-symmetric enzyme-active site in a single orientation, with the N-terminus of the inhibitor interacting with residues in monomer 2 of the enzyme and the C-terminus of the inhibitor interacting with residues in monomer 1. After extensive refinement of the structure, it became apparent that a second orientation of the inhibitor (with the inhibitor N- and C-termini interacting with monomers 1 and 2, respectively) was present. The two orientations of the inhibitor (which will be referred to as orientations 1 and 2) were originally given equal occupancy, but as refinement progressed the occupancies were adjusted in an attempt to equalize the mean thermal factor for the two orientations. The occupancies are 0.55 and 0.45 in the final model. There was no interpretable electron density for the morpholino group of the P_1' substituent and was therefore not possible to model the position of this group.

Results and Discussion

Consistent with the modeling observations, all inhibitors examined (**19**, **22–24**, and **29–45**) were highly potent in vitro with IC_{50}'s in the nanomolar range. Consequently, the para position on P_1 and P_1' can be viewed as essentially "neutral" to the thermodynamics of enzyme binding. As can be seen in Figure 4, the modeled structure of **29** is in good agreement with the subsequently determined X-ray structure. The hydrogen-bonding interaction predicted between the hydroxyl of the P_2' indanol and the NH of Asp_{29} is observed in the X-ray structure as shown in Figure 3 and Table VI. The only major difference between the two structures is in the orientation of the para substituent on the P_1' phenyl. This difference seems to be mostly due to a change in the position of the side chain of Arg_8 between the native and inhibited enzyme structures. This can be seen as a shift in the position of the "channel" which is occupied by this substituent in the active site of the native (Figure 5) and the inhibited (Figure 6) enzyme structures. Although only three atoms may be compared between the modeled and X-ray structures of **29** due to disorder in the X-ray structure at this position (vide supra), it is clear that the terminal methylene seen in the X-ray structure would have an unfavorable steric interaction with the native enzyme-active site. However, it is accommodated within the inhibited enzyme-active site.

The two orientations of the inhibitor observed in the X-ray structure have very similar backbone conformations (Table VI); greater torsional angle differences occur in the conformations of the P_1 and P_1' substituents. In both orientations, the inhibitory hydroxyl group is within hydrogen-bonding distance of all of the side-chain oxygens of the catalytic Asp-25 and Asp-225 residues (Table V). Two of the interactions between the inhibitor and the

---

(14) Fitzgerald, P. M. D.; McKeever, B. M.; VanMiddlesworth, J. F.; Springer, J. P.; Heimbach, J. C.; Leu, C.-T.; Herber, W. K.; Dixon, R. A. F.; Darke, P. L. Crystallographic Analysis of a Complex between Human Immunodeficiency Virus Type 1 Protease and Acetylpepstin at 2.0 Å Resolution. *J. Biol. Chem.* **1990**, *265*, 14209–19.

(15) Jaskolski, M.; Tomasselli, A. G.; Sawyer, T. K.; Staples, D. G.; Heinrikson, R. L.; Schneider, J.; Kent, S. B. H.; Wlodawer, A. Structure at 2.5 Å Resolution of Chemically Synthesized Human Immunodeficiency Virus Type 1 Protease Complexed with a Hydroxyethylene-Based Inhibitor. *Biochemistry* **1991**, *30*, 1600.

(16) Miller, M.; Schneider, J.; Sathyanarayana, B. K.; Toth, M. V.; Marshall, G. R.; Clawson, L.; Selk, L.; Kent, S. B. H.; Wlodawer, A. Structure of a Complex of Synthetic HIV-1 Protease with a Substrate-Based Inhibitor at 2.3 Å Resolution. *Science* **1989**, *246*, 1149.

(17) Erickson, J.; Neidhart, D. J.; VanDrie, J.; Kempf, D. J.; Wang, X. C.; Norbeck, D. W.; Plattner, J. J.; Rittenhouse, J. W.; Turon, M.; Wideburg, N.; Kohlbrenner, W. E.; Simmer, R.; Helfrich, R.; Paul, D. A.; Knigge, M. Design, Activity and 2.8 Å Crystal Structure of a C2 Symmetric Inhibitor Complexed to HIV-1 Protease. *Science* **1990**, *249*, 527.

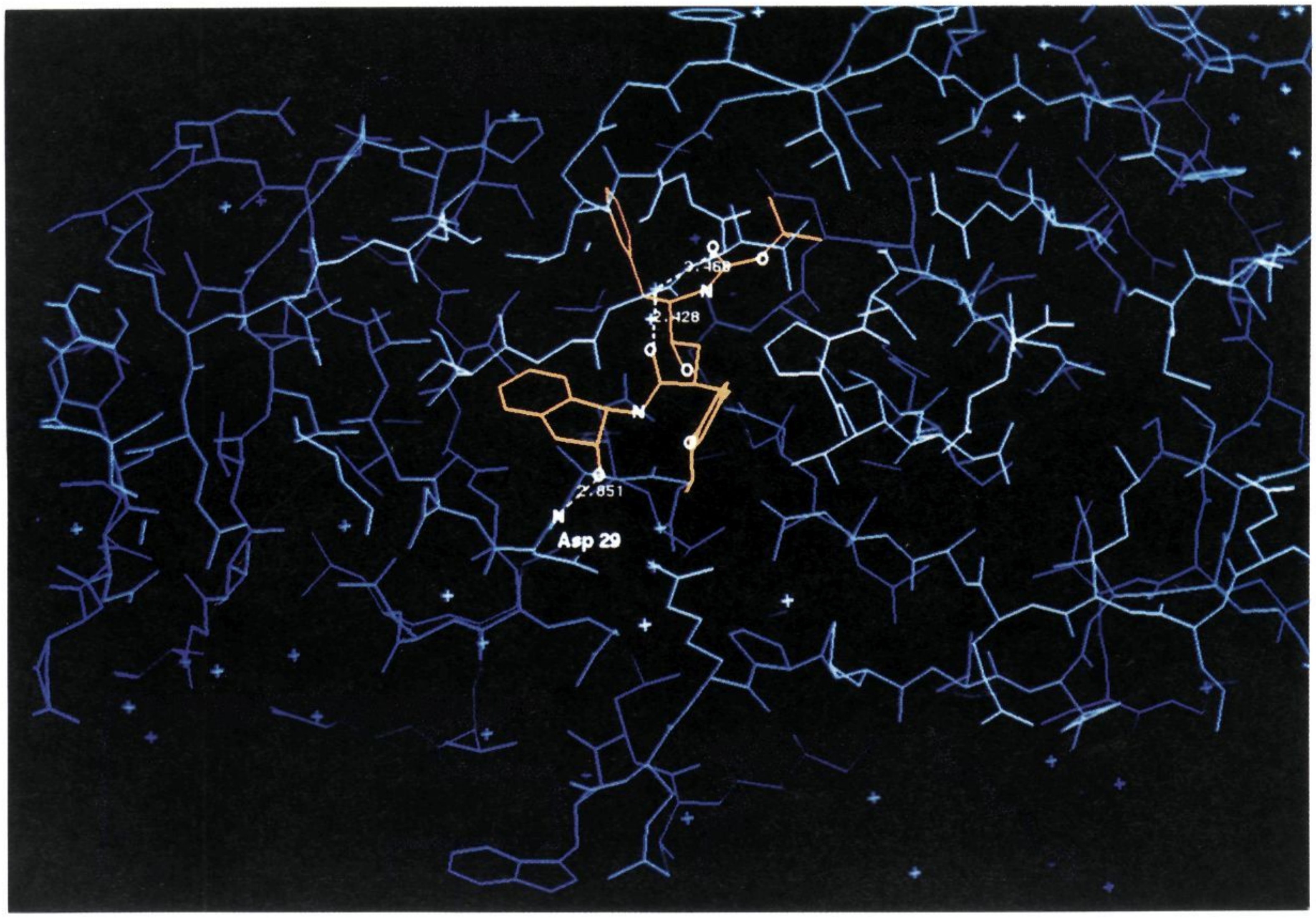

Figure 3. X-ray crystal structure of L-689,502-HIVP complex.

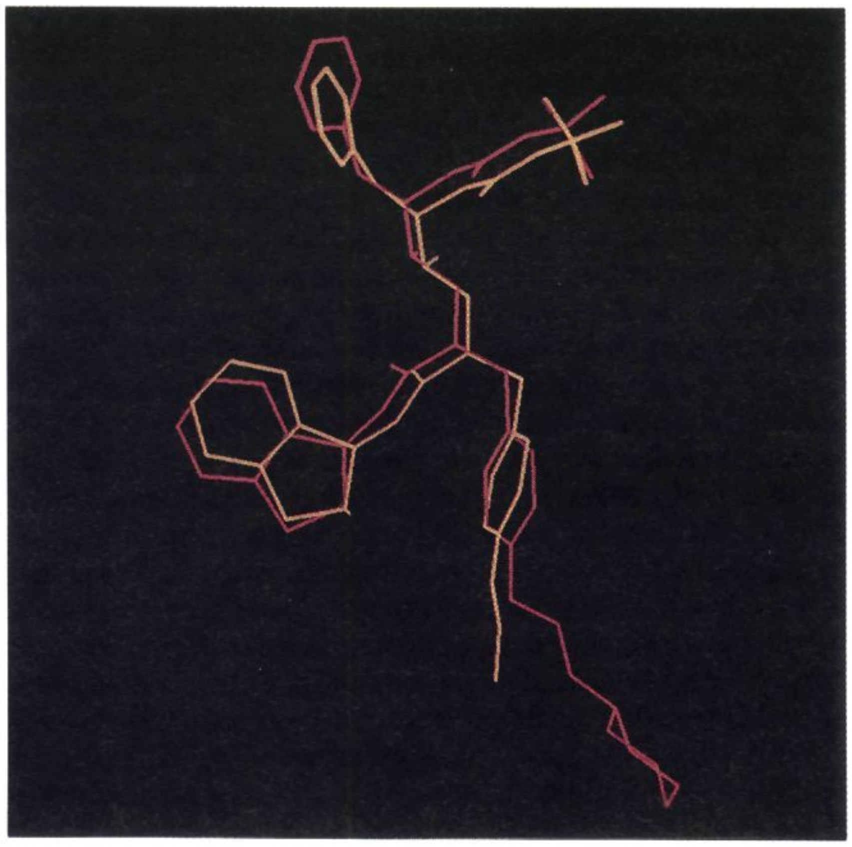

Figure 4. Comparison of L-689,502 active conformation as determined by modeling (red) and X-ray diffraction (yellow).

protein are mediated by solvent molecules. The tightly bound water that bridges between O_7 and O_{38} of the inhibitor and the amide nitrogens of Ile-50 and Ile-250 is analogous to a similar water molecule that has been observed in the previously determined structures of inhibited complexes of HIV-1 protease.[14-17] The second solvent-mediated interaction, bridging O_{42} of the inhibitor to the carbonyl oxygen of Gly-227 (or Gly-27) and to the side chain oxygens of Asp-229 (or Asp-29) has no analogue in the previously examined structures.

The increase in antiviral potency for **29** (L-689,502; CIC = 12 nM), relative to the decreased enzyme activity (IC_{50} = 0.45 nM) in comparison to the other inhibitors in Table I, may be due to the presence of the weakly basic morpholine group ($pK_a \sim 6.6$).[18] The highest value for the ratio of IC_{50} to CIC ($I/C = 0.0375$) observed in this series for L-689,502 is consistent with increased penetration into the HIV infected lymphocytes. In general, the presence of a weakly basic amine group (compounds **29–38**; $I/C > 0.004$) or *p*-oxygen substituent at P_1 or P_1' (compounds **19**, **22**, **23**, **44**, and **45**) enhanced the cell penetration relative to the parent compound 1 ($I/C > 0.003$). Increasing the basicity of the amine[19] (entries **33–36**) generally decreased the potency of the compound both as an enzyme inhibitor and antiviral agent relative to L-689,502.

While the double (P_1–P_1') hydroxylation in **24** was well tolerated by the HIV-1 protease enzyme (IC_{50} = 0.15 nM), the antiviral activity was markedly decreased (CIC = 780 nM) possibly as a result of increased acidity. In contrast, the bismorpholinyl compound **31** lost more than 10-fold in enzyme inhibitory potency (IC_{50} = 1.9 nM) and gained in cell penetration (CIC = 100 nM, $I/C = 0.02$), although to a lesser extent than one would expect if the effects were additive.

Not unexpectedly, the neutral hydroxyl or *N*-oxide functionalites in **41**, **44**, and **45** induced minimal effects

---

(18) The pK_a of **29** was determined by extrapolation of the pH vs solubility curve by Dr. Drazen Ostovic, Department of Pharmaceutical Research.

(19) Compounds **33–36** and **38** are expected to be more basic than **29** by comparison to the pK_a's of trimethylamine (9.8), *N*-methylpiperidine (10.2), *N*-methylpyrrolidine (10.2), *N,N'*-dimethylpiperazine (8.54), and *N*-methylmorpholine (7.13), taken from Dean, J. A. *Handbook of Organic Chemistry*; McGraw-Hill: New York, 1987; pp 8–2.

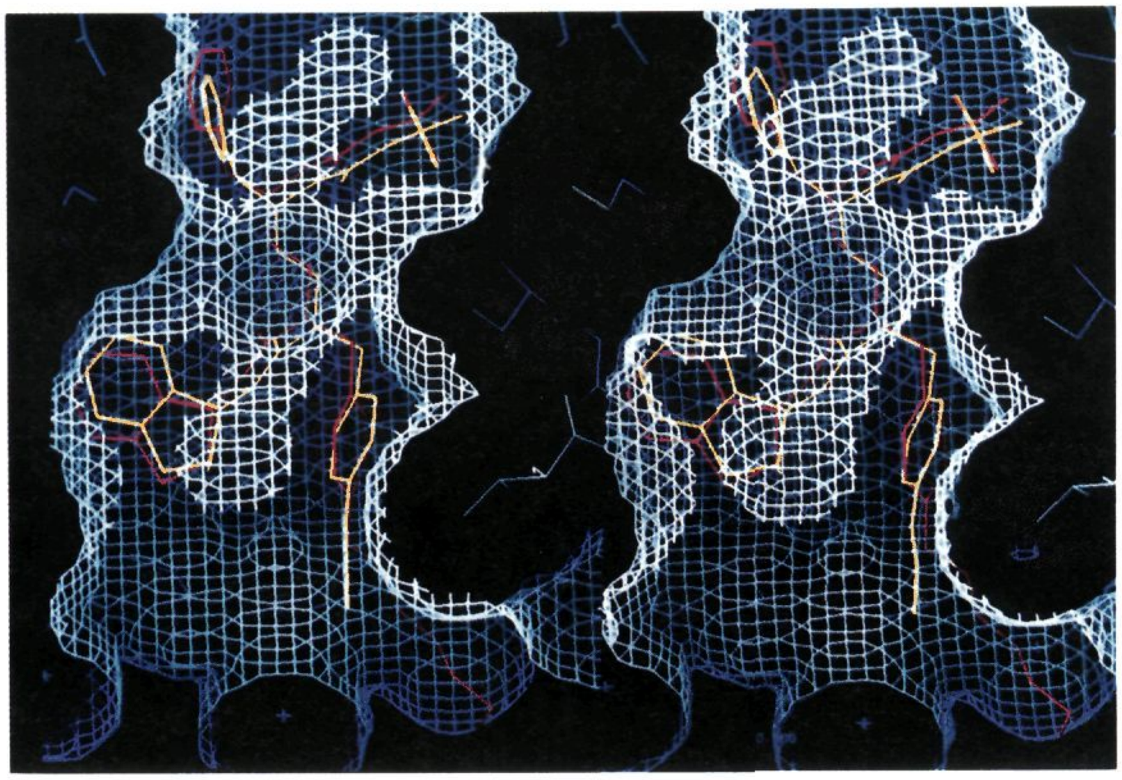

Figure 5. Comparison of L-689,502 active conformation determined by modeling (red) and X-ray diffraction (yellow) docked in native enzyme active site.

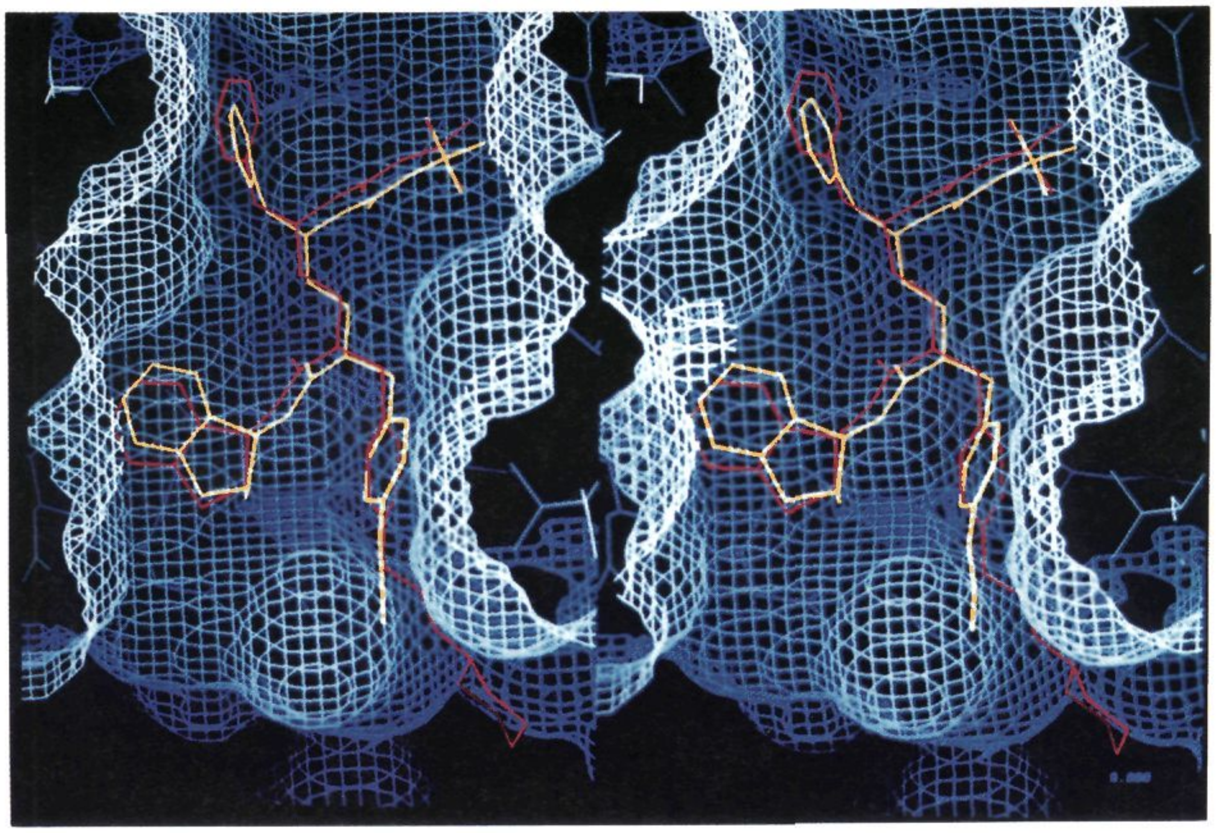

Figure 6. Active site of L-689,502 (red)–HIVP complex as determined by X-ray diffraction compared with active conformation of inhibitor from modeling (yellow).

on cell penetration ($I/C = 0.0072$, 0.004, and respectively vs 0.003 for the phenol **22**). The 2-hydroxyethyl ether group in **44** enhanced inhibitory activity against the retroviral protease which parallels the anti-HIV activity in cell culture. Finally, introduction of highly polar groups (entries **39**, **40**, and **43**) generally increased in vitro activity against HIV-1 protease concomitant with decreased cell penetration ($I/C < 0.003$) resulting in overall decreased antiviral activity.

Thus, attachment of 2-substituted ethoxy to the P_1' (or P_1) phenyl ring generally leads to overall enhancement of antiviral activity against HIV-1 in T-lymphoid cells through two possible mechanisms. When the 2-substituent is an electronegative group enhanced protease inhibition can give rise to increased antiviral activity. In the case of weakly basic amine groups, an increase in cell penetration may be responsible for increased blockade of viral spread.

The most potent compound in the series, L-689,502 was further evaluated for anti-HIV activity against five diverse strains of the HIV-1 and the SIV (simian immunodeficiency virus) in cell culture (Table II). At concentrations of 12–50 nM, L-689,502 completely prevented the spread of the virus in human H9 T-lymphoid cells. By contrast, in identical assays using the IIIb variant of HIV-1, the nucleoside analogues 3′-azidothymidine (AZT) and dideoxyadenosine (DDI) both exhibited CIC values of 25 mM. L-689,502 was also a potent inhibitor of HIV-1 infection spread in human MT-4 lymphoid cells, primary

---

(20) Henderson, L. E.; Benveniste, R. E.; Sowder, R.; Copeland, T. D.; Schultz, A. M.; Oroszlan, S. Molecular Characterization of *gag* Proteins from Simian Immunodeficiency Virus (SIV_{mne}.) *J. Virol.* **1988**, *62*, 2587–95.

(21) Heimbach, J. C.; Diehl, R. E.; Davis, L. J.; Deana, A. A.; Rooney, C. S.; Guare, J. P.; Giuliani, E. A.; Britcher, S. F.; Thompson, W. J.; Huff, J. R.; Kohl, N. E.; Darke, P. L. Analysis of Inhibitors of the HIV-1 Protease as HIV-2 Protease Inhibitors. Submitted to *Biochem. Biophys. Res. Commun.*

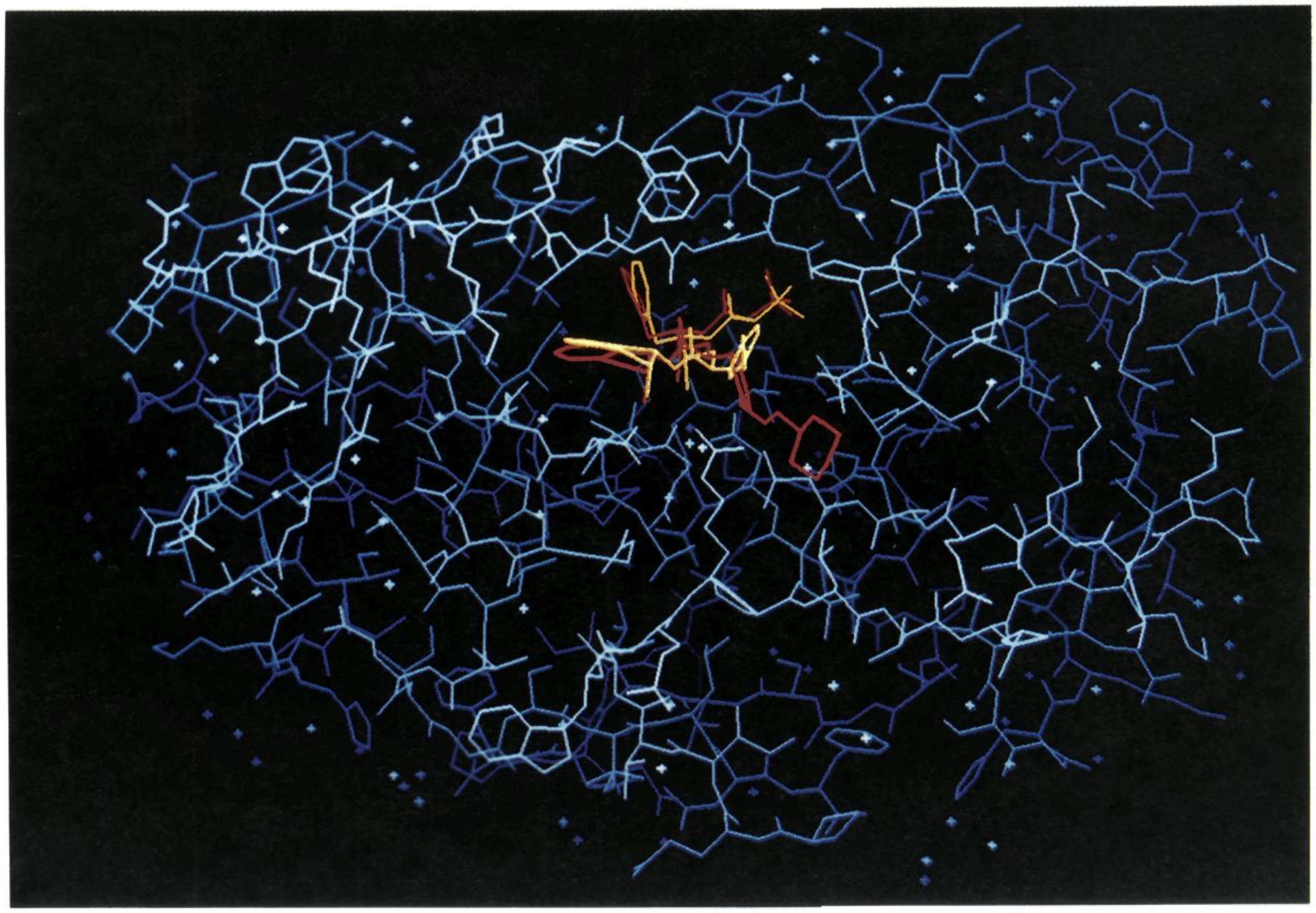

Figure 7. X-ray crystal structure of L-689,502 (red)–HIVP complex compared with active conformation of inhibitor from modeling (yellow).

Table II. Minimum Cell Culture Inhibitory Concentration (CIC) for Preventing Spread of HIV-1 and SIV Infection in Human Cells[a]

			CIC, nM	
compound	cell type	virus	fixed-cell immunofluorescence	p24-ELISA
L-689,502	MT-4 T-lymphoid	HIV-1 (IIIb)	25	6–50
L-689,502	peripheral blood lymphocytes	HIV-1 (IIIb)	0.78	12–25
L-689,502	monocytes/macrophages	HIV-1 (SF162)	25–50	
L-689,502	MT-4 T-lymphoid	HIV-1 (RF)	25–50	
L-689,502	MT-4 T-lymphoid	HIV-1 (MN)	25–50	
L-689,502	MT-4 T-lymphoid	HIV-1 (WMJ-2)	6–12	
L-689,502	MT-4 T-lymphoid	HIV-1 (RUTZ)	12	
L-689,502	H9 T-lymphoid	HIV-1 (IIIb)	6–12	12–25
AZT	MT-4 T-lymphoid	HIV-1 (IIIb)		25
DDI	H9 T-lymphoid	HIV-1 (IIIb)	25000	
L-689,502	H9 T-lymphoid	SIV (mac251)	800	
L-689,502	H9 T-lymphoid	SIV (mne)	200	

[a] Assay was performed as described in Experimental Section.

Table III. Data Measurement

shell		mean:	number of	number of	percent of	
min	max	$I/\sigma(I)$	observations	reflections[a]	possible data	R_{sym}[b]
∞	3.53	55.9	16465	3171	97.3	3.53
3.53	2.81	11.9	10694	2835	91.5	7.82
2.81	2.45	3.8	5270	2321	75.4	12.19
2.45	2.23	2.4	2068	1496	49.1	11.51
2.23	2.07	1.9	893	796	26.2	11.10
2.07	1.95	1.7	205	198	7.2	12.01
totals		20.8	35595	10817	59.2	5.69

[a] Only those reflections for which $I > s(I)$ were included in the data set. [b] $R_{sym} = \sum_n\sum_i|F_i - \langle F\rangle|/\sum_n\sum_i|\langle F\rangle|$, where F_i is the i-th observation of the n-th reflection and $\langle F\rangle$ is the mean of all observations of the n-th reflection.

peripheral blood lymphocytes, and primary peripheral monocytes/macrophages (Table II). In addition, L-689,502 inhibited cell culture infection by the SIV, albeit with a reduced potency. Due to the greater homology of the SIV and HIV-2 proteases,[20] a similar reduction in antiviral activity for L-689,502 would be expected for the latter virus. The lower K_i observed for L-689,502 against the HIV-2 protease confirms this prediction (K_i [HIV-1] = 0.2 nM; K_i [HIV-2] = 5.9 nM).[21] These results are consistent with the observed sequence differences for the HIV-1 and